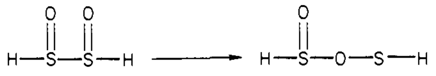

$$\underset{\mathbf{2}}{\mathrm{H{-}S({=}O){-}S({=}O){-}H}} \longrightarrow \underset{\mathbf{11}}{\mathrm{H{-}S({=}O){-}O{-}S{-}H}} \quad (10)$$

-45 kcal mol^{-1} (3-21G*), -28 kcal mol^{-1} (6-31G*)

$$\underset{\mathbf{11}}{\mathrm{H{-}S({=}O){-}O{-}S{-}H}} \longrightarrow \underset{\mathbf{10}}{\mathrm{H{-}O{-}S({=}O){-}S{-}H}}$$

-19.1 kcal mol^{-1} (3-21G*), -24.6 kcal mol^{-1} (6-31G*)

thermic by 43.8 kcal mol^{-1} at the 3-21G* level.

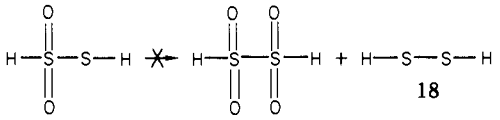

$$\underset{\mathbf{1}}{\mathrm{H{-}S(O_2){-}S{-}H}} \not\longrightarrow \underset{\mathbf{17}}{\mathrm{H{-}S(O_2){-}S(O_2){-}H}} + \underset{\mathbf{18}}{\mathrm{H{-}S{-}S{-}H}} \quad (12)$$

The sulfonyl radical (**15**), which is generally represented by three principal resonance contributors (eq 13), has been found

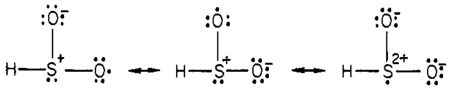

$$\underset{\mathbf{15}}{\mathrm{H{-}S^{+}(O^{-}){-}O\cdot}} \longleftrightarrow \mathrm{H{-}S^{+}(O\cdot){-}O^{-}} \longleftrightarrow \mathrm{H{-}S^{2+}(O^{-}){-}O^{-}} \quad (13)$$

to have hydrogen bonded to oxygen.[17,36-38] Moreover, although both HOSȮ and ROSȮ are known, alkyl sulfonyl radicals generally possess a carbon–sulfur single-bonded structure $\mathrm{R\dot{S}O_2}$.[36] Although sulfinyl radicals (**9**) are considered as stable, relatively

$$\underset{\mathbf{9}}{2\mathrm{HS\dot{O}}} \rightarrow \underset{\mathbf{15}}{\mathrm{HS\dot{O}_2}} + \underset{\mathbf{16}}{\mathrm{H\dot{S}}} \quad (14)$$

-13.6 kcal mol^{-1} (3-21G*)

delocalized, and unreactive π-type radicals,[13,16] the disproportionation of **9** to **15** and **16** appears to be thermodynamically favorable.

Conclusions

1. Although other reasonable mechanisms are possible, these theoretical calculations support the mechanism proposed for the rearrangement of α-disulfoxides (**2**) via sulfinyl radicals to thiosulfinates (eq 3–6). These calculations also suggest that α-disulfoxides (**2**) are sufficiently stable to be observed and/or isolated at low temperatures.[3,4]

2. The variation of the S–S bond lengths in **1–3**, **15**, and **16** agrees with the observed order of S–S bond homolysis for **1–3**, **15**, and **16**.

Recent low-temperature ^{1}H NMR and ^{13}C NMR studies show that the *m*-chloroperoxybenzoic acid oxidation of **2**-methyl-2-propyl 2-methyl-2-propanethiosulfinate (**23**)[3] and 2,2-dimethylpropyl 2,2-dimethylpropanethiosulfinate (**24**)[4] involves the corresponding α-disulfoxides (**25** and **26**) as intermediates. These resports represent the first direct observation of α-disulfoxide (**2**) intermediates.

$$\mathrm{R{-}S({=}O){-}S{-}R} \qquad \mathrm{R{-}S({=}O){-}S({=}O){-}R}$$

23, R = *t*-Bu **25**, R = *t*-Bu
24, R = *neo*-$\mathrm{C_5H_{11}}$ **26**, R = *neo*-$\mathrm{C_5H_{11}}$

Acknowledgement is made to the donors of the Petroleum Research Fund, administered by the American Chemical Society, for support of this research.

Registry No. 1, 80375-33-3; **1a**, 15060-43-2; **2**, 80375-34-4; **3**, 80375-36-6; **9**, 62470-71-7; **11**, 80375-38-8; **15**, 64255-60-3; **16**, 13940-21-1; **17**, 80375-39-9; **18**, 13465-07-1; **19**, 6481-73-8; **20**, 3347-03-3; **21**, 10409-06-0.

---

[36] Boyd, R. J.; Gupta, A.; Langler, R. F.; Lowrie, S. P.; Pencock, J. A. *Can. J. Chem.* **1980**, *58*, 331.

[37] Gilbert, B. C.; Kirk, C. M.; Norman, R. O. C. *J. Chem. Res. Synop.* **1977**, 173; *J. Chem. Res. Miniprint* **1977**, 1974.

[38] McMillan, M.; Waters, W. A. *J. Chem. Soc. B* **1966**, 422.

Al Atom–Ethylene and Al Atom–Acetylene Complexes: Matrix Isolation Electron Spin Resonance Study

Paul H. Kasai

Contribution from IBM Instruments, Inc., Danbury, Connecticut 06810.
Received August 31, 1981

Abstract: Al atom–ethylene and Al atom–acetylene complexes generated and/or trapped in rare-gas matrices at ~4 K were examined by ESR spectroscopy. The Al–monoethylene complex has a π-coordinated structure with a dative bond of donation from a semifilled p orbital of Al into the antibonding π orbital of ethylene. The Al atom and acetylene, in contrast, interact to form a σ-bonded adduct of vinyl structure. Photoirradiation of matrices containing Al–monoethylene complexes causes spectral changes suggesting the formation of Al–bis(ethylene) complexes. Photoirradiation of matrices containing the Al–acetylene adduct causes the cis–trans isomerization of the vinyl form.

Reactions between vaporized metal atoms and organic or inorganic molecules co-condensed at cryogenic temperature have been the subject of many recent investigations.[1] Skells and Wolf[2] demonstrated the formation of organoaluminum compounds when the aluminum atoms were co-condensed with excess propene or propyne at liquid-nitrogen temperature. Based upon the product analysis of the hydrolysis (by deuterium oxide) of the resultant organoaluminum compounds they concluded that the primary reaction between free aluminum atoms and alkene or alkyne molecules is an addition of one aluminum atom to the unsaturated bond. The structural feature of the primary product was not elaborated.

Recently we communicated to this journal the generation and detection by electron spin resonance (ESR) spectroscopy of Al atom–ethylene and Al atom–acetylene complexes in rare gas matrices.[3,4] The spectral analyses revealed that the Al atom–

---

[1] See, for example, a collection of review articles: *Angew. Chem., Int. Ed. Engl.*, **14**, 273 (1975).

[2] P. S. Skell and L. R. Wolf, *J. Am. Chem. Soc.*, **94**, 7919 (1972).

[3] P. H. Kasai and D. McLeod, Jr., *J. Am. Chem. Soc.*, **97**, 5609 (1975).

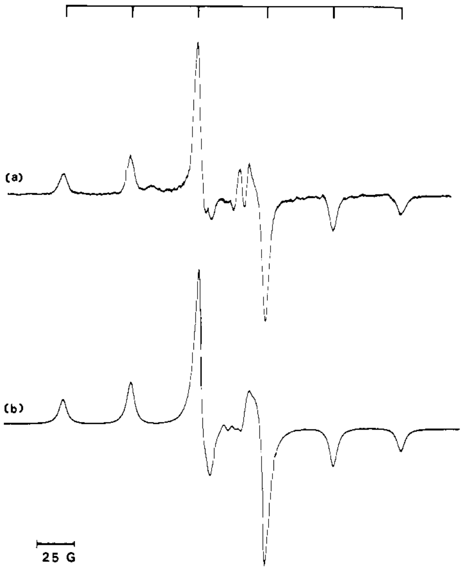

Figure 1. (a) ESR spectrum of Al atom–ethylene (C_2D_4) complexes generated in an Ar matrix. (b) A computer-simulated spectrum based on the parameters given in eq 1.

ethylene complex has a π-coordinated structure **1**, while the Al atom–acetylene system forms a σ-bonded adduct of vinyl structure **2**.

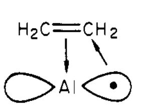

1

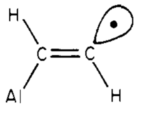

2

The purpose of this article is to present a more detailed account of the spectra of complexes **1** and **2**, and to report on interesting, if not fully understood, photoinduced spectral changes discovered and analyzed thenceforth. Photoirradiation of matrices containing **1** caused spectral changes that were strongly indicative of reactions involving a second ethylene molecule. Photoirradiation of matrices containing **2** induced the spectral change consistent with the cis–trans isomerization of the vinyl form.

Experimental Section

The basic design of the liquid helium cryostat-ESR spectrometer assembly that would permit condensation of high-temperature vapor-phase species in a rare-gas matrix and examination of the resultant matrix by ESR has been described earlier.[5] In the present series of study, the Al atoms were vaporized from a tantalum cell resistively heated to ~900 °C and were trapped in Ar or Ne matrices containing ethylene or acetylene (1–10 mol %). Perdeuterated ethylene, C_2D_4, and acetylene, C_2D_2 (enrichment >99%), were obtained from Merck and Company, Inc.

In the photoirradiation experiments the matrices were irradiated through a side quartz window, and a high-pressure Xe-arc lamp (Oriel, 1000-W unit) was used in combination with a set of sharp cut-off filters. The frequency of the ESR spectrometer locked to the sample cavity was 9.42 GHz and all spectra were observed while the matrices were maintained at ~4 K.

Spectra and Assignments

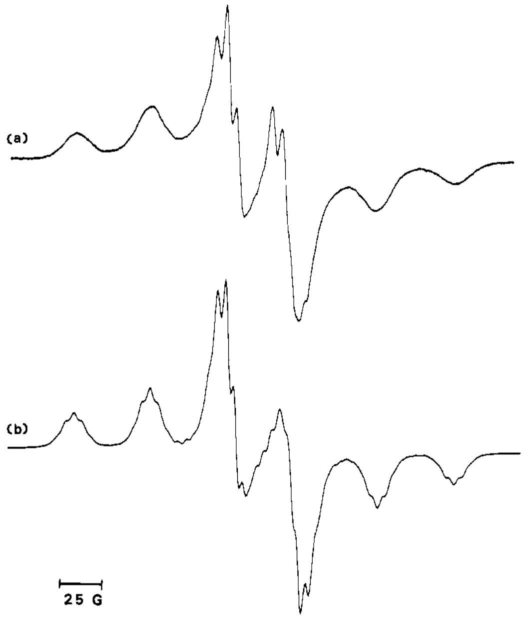

Figure 2. (a) ESR spectrum of Al atom–ethylene (C_2H_4) complexes generated in an Ar matrix. (b) A computer-simulated spectrum based on the parameters given in eq 1 and an isotropic coupling constant of 5 G with four equivalent protons.

Al Atom–Ethylene Complex. Both neon and argon matrices containing only Al atoms ($3s^23p^1$) appeared white and showed no ESR signal. The absence of the ESR signal attributable to Al atoms is due to extreme broadening caused by the degeneracy of the p orbitals.[6] The Ne and Ar matrices in which Al atoms were co-condensed with ethylene appeared green and showed an intense ESR signal possessing a unique symmetric pattern centered about the position corresponding to $g = 2.00$. Figures 1a and 2a show such spectra observed from Ar matrices containing Al and perdeuterioethylene (3%) and Al and normal ethylene (3%), respectively. These spectra are essentially identical with those of neon matrices observed and reported earlier.[3] When the ethylene concentration was varied from 1 to 3 to 10 mol %, the intensity of these spectra increased proportionately and no other signal appeared. The spectra are therefore assigned to the Al atom–monoethylene complex, $Al(C_2H_4)$.

The sharpening of the $Al(C_2H_4)$ spectrum upon deuteration is conspicuous. It is clear, however, that the prominent sextet pattern indicated in the figure must be attributed to the hyperfine interaction with the ^{27}Al nucleus (natural abundance = 100%, $I = {}^5/_2$). The unique line shape and the intensity pattern of the sextet can be accounted for by an extreme uniaxial nature of the coupling tensor ($|A_\parallel| \gg |A_\perp|$). Resorting to a method of computer simulation[7] via a trial-and-error procedure, the following g tensor and the Al coupling tensor were determined from the spectrum of the deuterated complex (Figure 1a). Figure 1b shows the

$$g_1 = 2.0097 \pm 0.0003 \qquad g_2 = 2.0025 \pm 0.0003$$
$$g_3 = 1.9965 \pm 0.0003$$
$$|A_1(\mathrm{Al})| = |A_3(\mathrm{Al})| = 5 \pm 1 \text{ G}$$
$$|A_2(\mathrm{Al})| = 44.5 \pm 0.5 \text{ G} \qquad (1)$$

computer-simulated spectrum based upon these parameters and a Lorentzian line shape with the line width of 6 G. Several computer-simulated spectra based on the g and/or the hyperfine coupling tensors slightly different from those given above are shown in Figure 3. The effect of the anisotropy of the g tensor upon the central region of the spectrum and the need for the nonzero perpendicular component of the hyperfine coupling tensor are clearly illustrated.

The partially resolved structure in the g_1 region of the $Al(C_2H_4)$ spectrum (Figure 2a) must surely be caused by the hyperfine interaction with the protons. A close inspection of the region revealed a structural pattern which is consistent with a hyperfine interaction of the magnitude ~5 G with four equivalent protons.

---

(4) P. H. Kasai, D. McLeod, Jr., and T. Watanabe, J. Am. Chem. Soc., **99**, 3521 (1977).

(5) P. H. Kasai, Acc. Chem. Res., **4**, 329 (1971).

(6) The spectrum due to Al atoms has been seen in heavily concentrated matrices where the degeneracy of the 3p orbitals is removed by the lattice distortions. J. H. Ammeter and D. C. Schlosnagle, J. Chem. Phys., **59**, 4784 (1973).

(7) P. H. Kasai, J. Am. Chem. Soc., **94**, 5950 (1972). A high nuclear spin ($I = {}^5/_2$) of Al and large hyperfine interaction with it necessitated inclusion of the second-order terms in the simulation program.

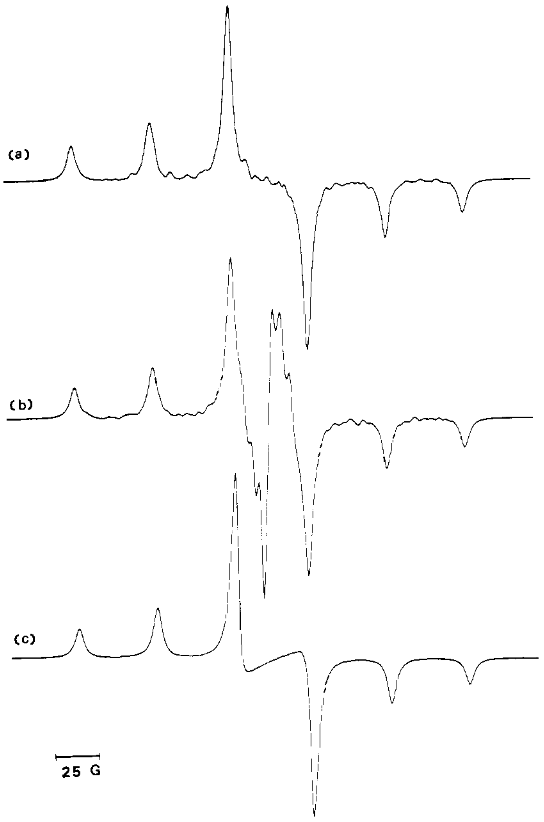

Figure 3. Computer-simulated spectra of Al(C_2D_4) assuming $A_\parallel$ = 44.5 G and: (a) an isotropic g (2.0023) and $A_\perp$ = 0, (b) an isotropic g (2.0023) and $A_\perp$ = 5 G, and (c) an orthorhombic g (as given in the text) and $A_\perp$ = 0.

Figure 2b shows the computer-simulated spectrum based upon the g tensor and the Al coupling tensor assessed above and an isotropic hyperfine coupling interaction of 5 G with four equivalent protons. The agreement between the observed and simulated spectra is reasonable; the small discrepancy is believed to result from the neglect of the anisotropy of the proton coupling tensors and the staggered orientations of their principal axes.

Photoinduced Reactions in Al/C_2H_4/Ar Matrices. Most interestingly, we found that the ESR spectra of the matrices discussed above changed drastically when irradiated with light. As stated earlier the color of a matrix containing Al and ethylene is green. The sequence Figure 4a→4b illustrates the spectral change observed when the Al/C_2D_4(5%)/Ar system was irradiated with visible light (λ > 4000 Å). The corresponding photoinduced change observed with the Al/C_2H_4(5%)/Ar system is shown in Figure 5a→5b. The change was gradual but complete in about 20 min for matrices with high ethylene concentration (≥2%). When the ethylene concentration was low (≤1%) a significant fraction of the original spectrum remained unaltered. The species responsible for the visible-light-induced spectra (Figures 4b and 5b) were found to be stable against UV light (4000 Å > λ > 3000 Å). No further spectral change was observed when the matrices that had been irradiated with visible light were subsequently exposed to UV irradiation.

Curiously though, when the original matrices containing Al and ethylene were subjected to UV irradiation immediately, totally different spectral changes occurred. See sequences in Figures 4a→4c and 5a→5c. A close inspection of the UV-induced spectrum of the Al/C_2D_4/Ar system (Figure 4c) reveals the presence of the spectral pattern identifiable as that seen in the visible-light-induced spectrum (Figure 4b), and also weak signals due to deuterium atoms. The spectrum, however, is dominated by the strong central signal of a new, UV-induced species. The widely spaced multiplet prominent in the UV-induced spectrum of Al/C_2H_4/Ar (Figure 5c) is thus attributed to the proton hyperfine structure of the new species. Again when the ethylene concentration was low (≤1%) a significant fraction of the original spectrum remained unchanged.

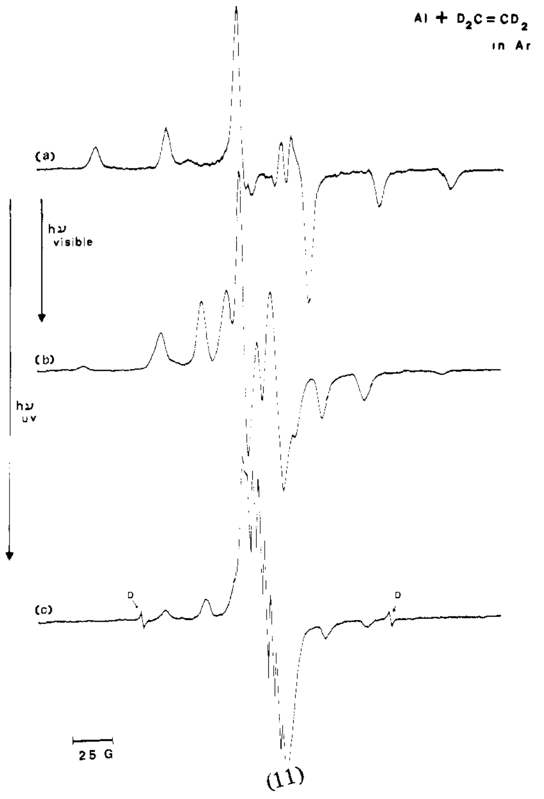

Figure 4. ESR spectra of the Al/C_2D_4/Ar system observed: (a) as prepared, (b) after irradiation with visible light (λ > 4000 A), and (c) after irradiation with UV light.

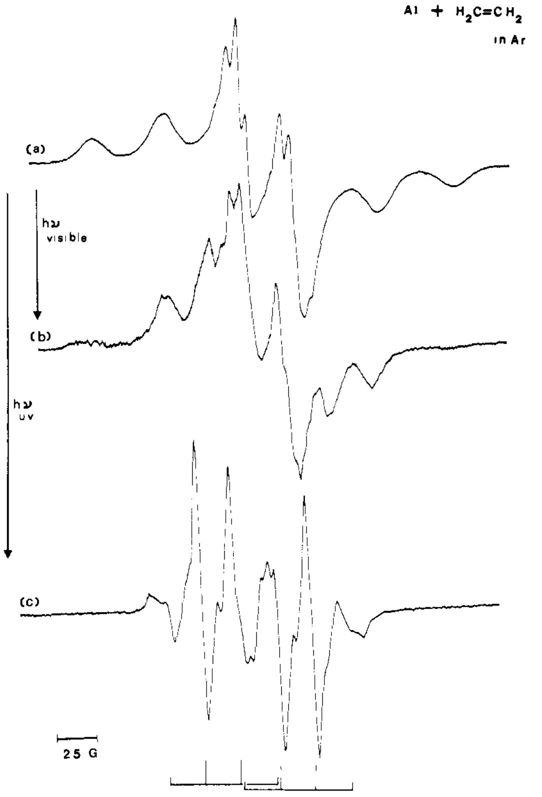

Figure 5. ESR spectra of the Al/C_2H_4/Ar system observed: (a) as prepared, (b) after irradiation with visible light (λ > 4000 A), and (c) after irradiation with UV light.

The overall patterns of the original spectra (Figures 4a and 5a) and those of the visible-light-induced spectra (Figures 4b and 5b)

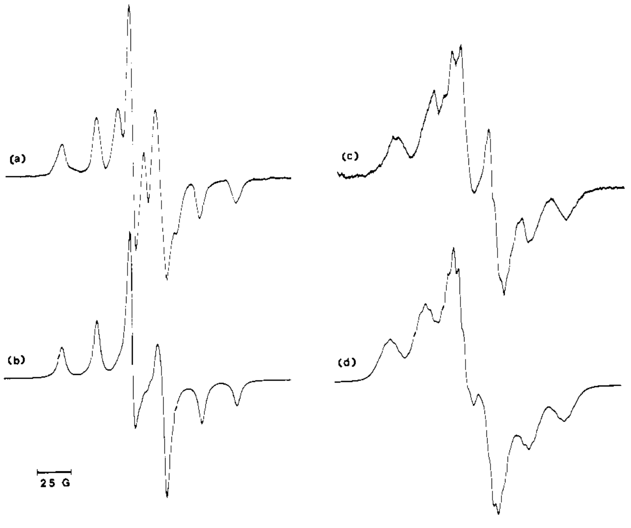

Figure 6. Visible-light-induced ESR spectra of the Al/ethylene/Ar system: (a) observed from Al/C_2D_4/Ar, (b) computer simulated based upon the parameters given in eq 2, (c) observed from Al/C_2H_4/Ar, and (d) computer simulated based on the parameters given in eq 2 and an isotropic coupling constant of 4 G with eight equivalent protons.

are similar. Hence the latter spectra are also characterized by an Al coupling tensor of uniaxial symmetry and a small, unresolved hyperfine coupling interaction with protons. The magnitude of the Al coupling tensor, however, is reduced to $\sim{}^1/_2$ of the original species. With use of the method of computer simulation the g tensor and the Al coupling tensor of the visible-light-induced species were assessed as follows:

$$\begin{gathered} g_1 = 2.0083 \pm 0.0003 \qquad g_2 = 2.0023 \pm 0.0003 \\ g_3 = 1.9993 \pm 0.0003 \\ |A_1(\mathrm{Al})| = |A_3(\mathrm{Al})| = 4.0 \pm 0.5 \text{ G} \\ |A_2(\mathrm{Al})| = 25.5 \pm 0.5 \text{ G} \end{gathered} \tag{2}$$

The observed, visible-light-induced spectra and the computer-simulated spectra based upon these parameters are compared in Figure 6. In simulating the spectrum of the species involving C_2H_4, an isotropic coupling interaction of 4 G with eight equivalent protons was assumed. The rationale for this assumption will be discussed later.

The most notable feature of the UV-induced spectra (Figures 4c and 5c) is the apparent lack of hyperfine structure due to the Al nucleus. The widely spaced multiplet in Figure 5c was recognized as an overlapping doublet of quartets as indicated. The quartets have the relative intensity expected from the interaction with three equivalent protons. Resorting to the method of spectral simulation the g tensor, the coupling tensor to the unique proton, and those to the three equivalent protons were determined as follows:

$$\begin{array}{llll} & x & y & z \\ g & 2.0023 & 2.0023 & 2.0023 \\ \mathrm{H(1)} & 44 \pm 1 \text{ G} & 49 \pm 1 \text{ G} & 45 \pm 1 \text{ G} \\ \mathrm{H(3)} & 29 \pm 1 \text{ G} & 18 \pm 1 \text{ G} & 18 \pm 1 \text{ G} \end{array} \tag{3}$$

The observed spectra and the computer-simulated spectra based upon these parameters are compared in Figure 7.

Al Atom–Acetylene Adducts. Figures 8a and 9a show the ESR spectra observed when Al atoms were condensed in neon matrices together with perdeuterioacetylene and normal acetylene, respectively. As in the case of Al and ethylene, these are the only signals observed, and their intensities increased proportionately with increasing acetylene concentration. They are thus attributed to aluminum–monoacetylene species.

The sextet feature clearly resolved in the Al/C_2D_2/Ne system (Figure 8a) is attributed to the hyperfine structure due to ^{27}Al. We note that, in contrast to the Al coupling tensor observed with the Al–ethylene system, the Al coupling tensor seen here is essentially isotropic. The successive outward increase in the line width of each hyperfine component indicates the presence of small anisotropy, however.

Figure 7. UV-light-induced ESR spectra of the Al/ethylene/Ar system: (a) observed from Al/C_2D_4/Ar, (b) computer simulated based on the parameters given in eq 3 with appropriate corrections for deuteration, (c) observed from Al/C_2H_4/Ar, and (d) computer simulated based on the parameters given in eq 3.

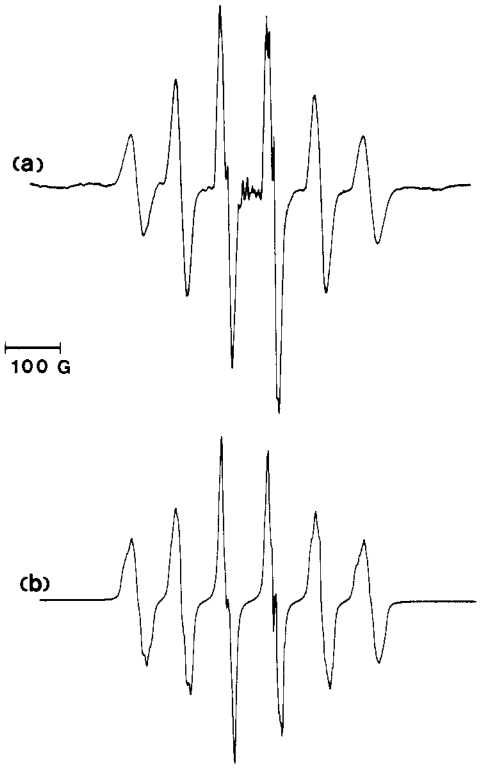

Figure 8. ESR spectra of the Al/acetylene/Ne system: (a) observed from Al/C_2D_2/Ne, and (b) computer simulated based on the parameters given in eq 4 with appropriate corrections for deuteration.

The complex but well-resolved spectral pattern seen in Figure 9a must result from additional coupling interactions with the protons. A close inspection of the central section of the spectrum reveals the presence of several doublet-of-doublet patterns spaced by the Al coupling constant as indicated. The spacings of the doublets are ~55 G and ~20 G, respectively. The patterns in the outer regions are obscured by the increased effect of the anisotropy of the Al coupling tensor.

The magnitudes and the symmetry characteristics of the hyperfine coupling tensors delineated above with one aluminum nucleus and two nonequivalent protons suggest that the observed

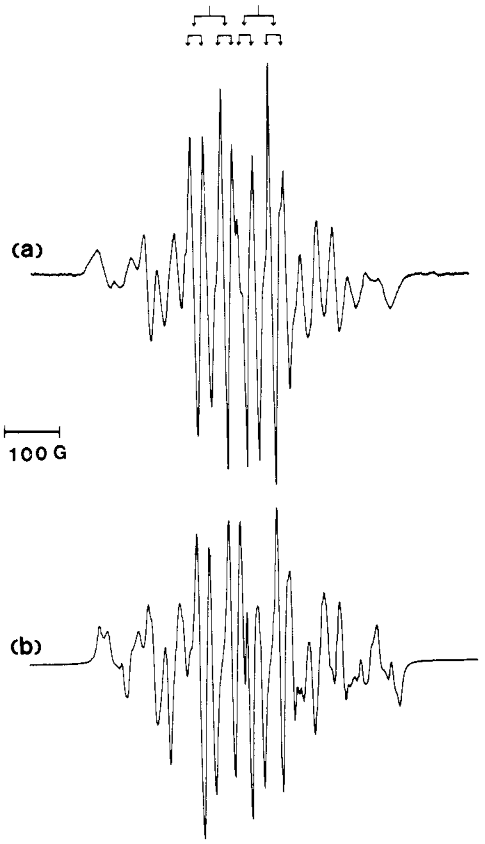

Figure 9. ESR spectra of the Al/acetylene/Ne system: (a) observed from Al/C_2H_4/Ne, and (b) computer simulated based on the parameters given in eq 4.

spectra be assigned to the Al-acetylene *adduct* having the vinyl structure. The larger doublet splitting of ~55 G is attributed

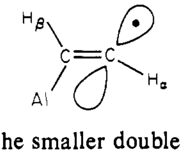

to the β proton, and the smaller doublet splitting of ~20 G to the α proton. A larger hyperfine interaction is expected from the β proton because of a direct overlap possible between its 1s orbital and the nonbonding semifilled orbital at the α carbon. Again, via the trial-and-error computer spectral simulation, the g and hyperfine coupling tensors were determined as follows:

	x	y	z	
g	2.005	2.0023	2.0023	
Al	85 ± 1 G	92 G	78 G	(4)
H_α	25	20	15	
H_β	55	55	55	

Figures 8b and 9b are the computer-simulated spectra based upon these parameters.

In preparing the rare-gas matrices containing metal atoms and gaseous molecules such as ethylene or acetylene, the gaseous molecules can be introduced either premixed with rare gas prior to deposition or separately through the vapor sample inlet. The design of our cryostat is such that, in the latter mode of operation, the metal atoms traverse through the ethylene or acetylene vapor prior to condensation. In the case of Al and ethylene the identical spectral results were obtained in either mode of operation. In the case of Al and acetylene only the latter, "vapor phase" mode resulted in matrices showing the spectrum of significant intensity. It is thus concluded that Al and acetylene do not react in matrices at ~4 K. That some thermal activation energy is required for the production of Al-acetylene adduct is not surprising since it entails the breakup of a π bond of acetylene.

Photoisomerization of Al-Acetylene Adducts. Neon matrices in which Al and acetylene had been co-condensed appeared purple.

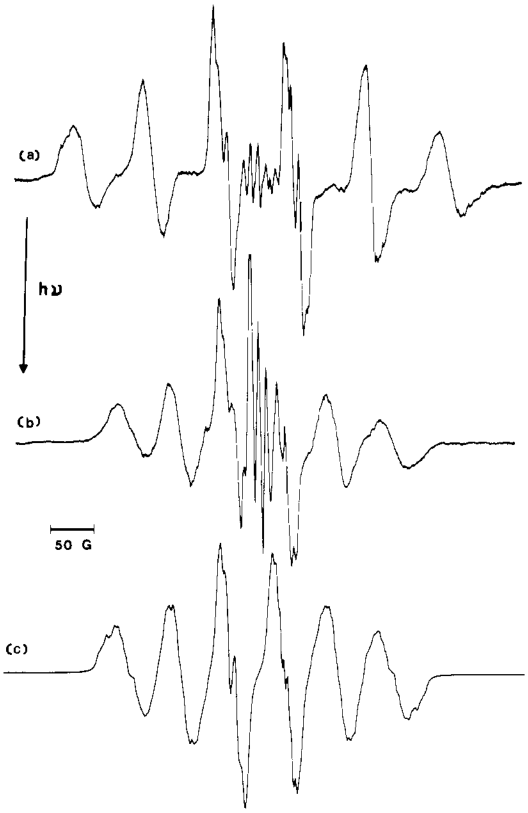

Figure 10. ESR spectra of Al(C_2D_2): (a) observed as prepared, (b) observed after irradiation with visible light (λ > 4000A), and (c) computer simulated based on the parameters given in eq 5 with appropriate corrections for deuteration.

Subsequent irradiation of the matrices with visible light (λ > 4000 Å) brought about the spectral changes illustrated in Figures 10 and 11. The change was gradual but complete in about 20 min.

A careful comparison of the original and the photoinduced spectra led us to conclude that the latter spectra were also characterized by the hyperfine coupling tensors with one aluminum nucleus and two nonequivalent protons quite similar to those determined from the original spectra. The observed, rather dramatic spectral changes are due primarily to a decrease in the magnitude of the Al coupling interaction and an increase in its anisotropy. We suggest that the photoconversion results from the cis-trans isomerization of the vinyl form.

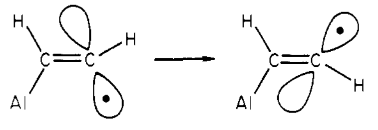

The g tensor and the coupling tensors of the photoinduced species were assessed as follows:

	x	y	z	
g	2.0023	2.0023	2.0023	
Al	70 ± 1 G	60 ± 1 G	50 ± 1 G	(5)
H_α	26 ± 5	26 ± 5	26 ± 5	
H_β	56 ± 1	56 ± 1	56 ± 1	

The coupling tensor to the α proton is expected to have an anisotropy similar to that detected for the α proton of the original species. However, its assessment was made difficult by the increased anisotropy of the Al coupling tensor. Figures 10c and 11c show the computer-simulated spectra based upon these parameters.

Essentially identical spectral changes were observed when the original matrices were irradiated with UV light (λ > 3000 Å). The only notable difference was an increased intensity (×2) of the sharp triplet seen in Figure 10b near the center of the spectrum. The triplet has a spacing of ~9 G and is presumably caused by

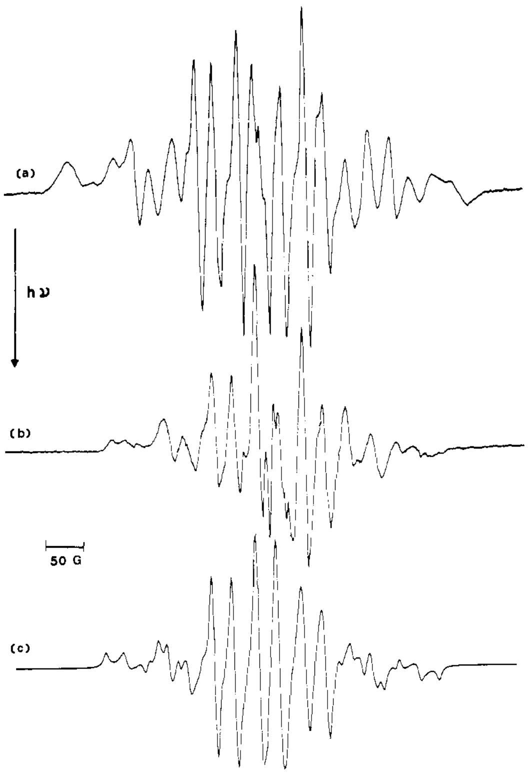

Figure 11. ESR spectra of $Al(C_2H_2)$: (a) observed as prepared, (b) observed after irradiation with visible light (λ > 4000 Å), and (c) computer simulated based on the parameters given in eq 5.

the interaction with a deuterium nucleus. No signal with the corresponding doublet spacing was recognized in the spectrum of the UV-irradiated $Al/C_2H_2/Ne$ system, however. The identity of this deuterium-related triplet has not been established.

Structures and Discussions

For a complex formed between an olefinic system and a neutral Al atom ($3s^23p^1$), we may envisage one of the following modes of interactions.

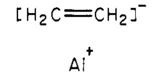

I

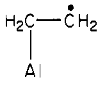

II

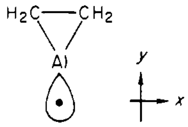

III

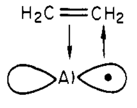

IV

I represents the interaction of a charge-transfer complex. In II a metal–carbon σ bond is formed and the unpaired electron is localized at the terminal carbon. III invokes an sp^2 hybridization of Al, and the formation of an alumina–cyclopropane ring; the unpaired electron is in an sp^2-hybridized orbital pointing away from the ethylene moiety. IV invokes an sp_y hybridization of Al, and the complex is formed by two dative bonds, one resulting from migration of electrons from the bonding π orbital into the vacant sp_y orbital of Al and the other of "back donation" from the semifilled p_x orbital of Al into the vacant antibonding π orbital.

Let us discuss the structure of the Al–monoethylene complex examined in the preceding section. The small proton coupling constant and the substantial interaction with the Al nucleus rule out I and II immediately. If the g tensor of a radical deviates little from that of a free electron, and the distribution of the unpaired electron in the immediate vicinity of a magnetic nucleus is axially symmetric, the principal hyperfine coupling constants to the magnetic nucleus can be shown to be related to the isotropic term A_{iso} and the anisotropic, dipolar term A_{dip} as follows:

$$A_{\parallel} = A_{iso} + 2A_{dip} \qquad A_{\perp} = A_{iso} - A_{dip} \tag{6}$$

where $A_{iso} = g_e\beta_e g_n\beta_n(8\pi/3)|\Phi(0)|^2$ and $A_{dip} = g_e\beta_e g_n\beta_n\langle(3\cos^2\theta - 1)/2r^3\rangle$. Here $|\Phi(0)|^2$ represents the spin density at the magnetic nucleus, r the separation between the unpaired electron and the magnetic nucleus, and θ the angle between r and the symmetry axis.[8]

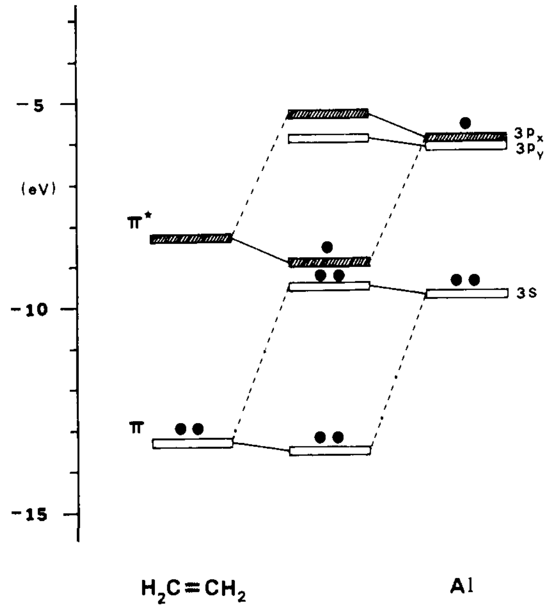

Figure 12. Schematic energy diagram showing the interaction of the π and π* orbitals of ethylene with the valence orbitals of Al leading to the formation of the π-coordinated complex.

In both III and IV, the distribution of the unpaired electron around the Al nucleus is axially symmetric, and the A_{iso} and A_{dip} terms of the Al coupling tensor should arise from the spin densities in the Al 3s and 3p orbitals, respectively. The analysis of the observed coupling constants (eq 1) of $Al(C_2H_4)$ according to eq 6 yields the following: if $A_{\parallel} > 0$ and $A_{\perp} > 0$, $A_{iso} = 18.2$ G and $A_{dip} = 13.2$ G; and if $A_{\parallel} > 0$ and $A_{\perp} < 0$, $A_{iso} = 11.5$ G and $A_{dip} = 16.5$ G. The magnitudes of A_{iso} and A_{dip} expected from a unit spin density in the Al 3s and 3p orbitals have been estimated to be 985 and 21 G, respectively.[9] We thus note that the spin density in the Al 3s orbital is extremely small (1.8 or 1.2%) while the spin density in the 3p orbital is large (63 or 79%). We conclude that the $Al(C_2H_4)$ complex observed here results from the bonding scheme IV. The small A_{iso} revealed above is then attributed to the spin density induced in the filled s orbitals of Al through a polarization process.

The LCAO molecular orbital description of the semifilled orbital in the bonding structure IV would be

$$\Phi = a[p_x(\mathrm{Al})] + b[p_y(C_1) - p_y(C_2)] \tag{7}$$

If $a^2 = 0.63$ (as determined above assuming $A_{\parallel} > 0$ and $A_{\perp} > 0$), one obtains $b^2 \simeq 0.2$. If the ethylene moiety in the complex is to retain the planar structure, McConell's relation then predicts the proton hyperfine interaction of ~4.6 G in close agreement with the value assessed from the observed spectrum.

The EHT (extended Hückel theory) molecular orbital calculation places the bonding and antibonding π orbitals of ethylene at −13.2 and −8.2 eV, respectively. Figure 12 depicts schematically the π orbital levels of ethylene, the relevant valence orbitals of the Al atom, and their correlations to the pertinent levels of the Al–monoethylene complex. The exact energy levels of the complex are not known; they are drawn in the figure to indicate their positions relative to the interacting orbitals of Al and C_2H_4. The figure indicates that the dative bond of "forward donation", the migration of bonding π electrons into the sp_y orbital of Al, is probably insignificant. The one-electron dative bond of "back

---

(8) For the analyses of hyperfine coupling tensors, see, for example, P. W. Atkins and M. C. R. Symons, "The Structure of Inorganic Radicals", Elsevier, Amsterdam, 1967.

(9) J. R. Morton, J. R. Rowlands, and D. H. Whiffen, *Natl. Phys. Lab., Gr. Brit.*, No. **BPR13**. Also see ref 8, p 21.

donation" must be primarily responsible for the formation of the complex.

It is interesting that the Al atom and acetylene molecule encountered within the matrix do not form the complex of this type, although the energy levels of the π orbitals of acetylene are very similar to those of ethylene. In the molecular geometry instigated by IV the overlap between the Al p_x orbital and the antibonding π orbital of the olefinic system would be sensitive to the C–C distance. A shorter C–C distance of acetylene must adversely affect this overlap to such an extent that the complex is no longer stable. We have shown recently that the Al atom complexes with benzene interacting through one C=C unit of the ring, and that its one-electron dative bond can be described by an equation entirely analogous to eq 7.[10] For the Al atom-benzene complex, however, it was determined that $a^2 \simeq 0.2$ and $b^2 \simeq 0.4$, indicating the electron migration of a much further extent. The C–C bond distance of benzene is longer than that of ethylene.

As stated earlier, higher ethylene concentration was found to be conducive for the photoinduced spectral changes observed in the Al/C_2H_4/Ar system. Photoinduced reactions between the Al-monoethylene complex and second ethylene molecule are thus strongly suggested. We have shown recently that both Cu and Ag atoms interact with two ethylene molecules in rare-gas matrices and form planar bis(ethylene) complexes depicted below.[11]

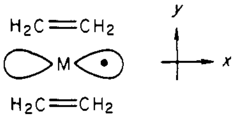

3

The electronic configurations of Cu and Ag atoms are $(n-1)d^{10}ns^1$. In these bis(ethylene) complexes the unpaired electron is promoted to the np_x orbital and forms the dative bond given by

$$\Phi = a\Phi_M(p_x) + b(\pi_1^* - \pi_2^*) \qquad (8)$$

where π_1^* and π_2^* represent, respectively, the antibonding π orbitals of the ethylene molecules.

We suggest that the spectra (Figures 4b and 5b) induced by visible light in the Al/C_2H_4/Ar system are due to Al$(C_2H_4)_2$ of the structure similar to those of Cu- and Ag-bis(ethylene) complexes. The semifilled orbital of the envisaged Al-bis(ethylene) complex would also be given by eq 8. The Al coupling tensor (eq 2) of the visible-light-induced species with the uniaxial symmetry similar to that of Al-monoethylene complex, but significantly reduced in overall magnitude, is thus accounted for. The analysis of the Al coupling tensor, following the procedure performed for Al(C_2H_4) and assuming $A_\parallel > 0$ and $A_\perp > 0$, yields $a^2 \simeq 0.36$. This leads to the spin density of ~0.16 in the p_y orbital of each carbon and hence the proton coupling constant of ~3.7 G. The g tensor and the Al coupling tensor assessed from the deuterated species and the isotropic coupling constant of 4 G with eight equivalent protons generate the simulated spectrum shown in Figure 6d.

In the cases of Cu/C_2H_4/Ar and Ag/C_2H_4/Ar systems, the bis(ethylene) complexes were spontaneously formed in matrices with higher ethylene concentration (>1%). It is not unexpected that the barrier for diffusion in rare-gas matrices would be higher for Al atoms of the ^{2}P state than for Cu or Ag atoms of the ^{2}S state. We suggest, in the case of Al/C_2H_4/Ar, that the formation of bis(ethylene) complex becomes possible when the barrier for diffusion is lowered by irradiation with visible light.

As stated earlier, the spectra induced by "direct" UV irradiation in the Al/C_2H_4/Ar system show no discernible structure due to Al. The 1:3:3:1 quartet feature with the average coupling constant of 22 G suggests the presence of a methyl group adjacent to a localized radical center. The large, essentially isotropic doublet splitting of ~46 G is suggestive of a β proton in vinyl radicals. The UV-induced spectra are therefore tentatively attributed to α,β-dimethylvinyl radical 4.

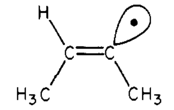

4

Many reaction sequences that would generate radical 4 from Al(C_2H_4) and a second ethylene molecule may be conjectured. One such sequence is shown below.

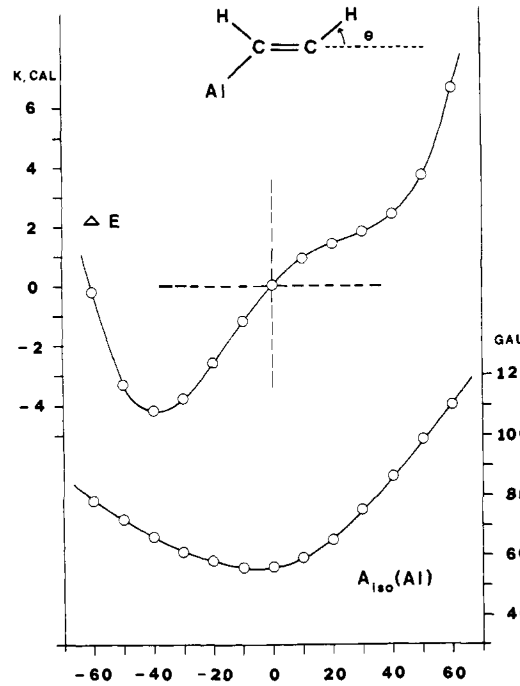

Figure 13. Dependency of the total energy and the aluminum A_{iso} of Al(C_2H_2) upon θ (the angle of bend of the C=C$_\alpha$—H$_\alpha$) determined by an EHT molecular orbital calculation.

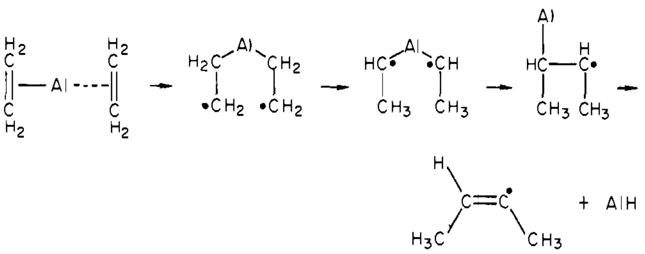

The last step, removal of AlH, is a well-known β-elimination process of metal σ-hydrocarbyls. However, both the assignment of the spectra to radical 4 and the reaction sequence suggested above for its generation are highly speculative, and should be regarded with due reservation.

The formation of the Al-acetylene adduct having the vinyl structure is clearly an example of the interaction scheme II. That this vapor-phase reaction occurs between Al and acetylene but not between Al and ethylene must signify the difference in the energetics involved. The bond strength of the Al–C σ bond is thus estimated to be larger than 50 kcal (the difference between the carbon–carbon triple and double bonds) but less than 65 kcal (the difference between the carbon–carbon double and single bonds).

For the unsubstituted vinyl radical, $H_2C=\dot{C}H$, it has been shown that the coupling constant to the α proton is positive and that its C=C$_\alpha$—H$_\alpha$ section is bent.[12] For the Al-acetylene adduct

---

[10] P. H. Kasai and D. McLeod, Jr., *J. Am. Chem. Soc.*, **101**, 5860 (1979).

[11] P. H. Kasai, D. McLeod, Jr., and T. Watanabe, *J. Am. Chem. Soc.*, **102**, 179 (1980).

[12] E. L. Cochran, F. J. Adrian, and V. A. Bowers, *J. Chem. Phys.*, **40**, 213 (1964). See also ref 7.

2 the essentially isotropic interaction with Al is the result of direct overlap possible between its 3s orbital and the semifilled orbital of the α carbon. The sign of the Al coupling elements given in eq 4 must therefore be positive. The z axis along which the smallest Al coupling constant is measured must then be perpendicular to the molecular plane. The smallest α-proton coupling constant was also observed along the z axis. It follows that the α-proton coupling constant of the Al–acetylene adduct is positive and its $C{=}C_\alpha{-}H_\alpha$ section is also bent.

As stated earlier the photoinduced spectral change observed with the $Al/C_2H_2/Ar$ system can be best understood in terms of the cis–trans isomerization of the vinyl form. We therefore examined the radical **2** by the EHT (extended Huckel type) molecular orbital theory. In particular, based on the structural parameters depicted below, the total energy of the radical and the isotropic Al coupling constant were examined as a function of θ, the angle of bend of the $C{=}C_\alpha{-}H_\alpha$ section. The results are shown in Figure 13. The EHT-MO theory thus states that the trans configuration at $\theta \simeq -40°$ is more stable than the linear structure ($\theta = 0°$) by ~4 kcal. The energy vs. θ curve does not show a minimum in the $\theta > 0$ region; its shape, however, strongly suggests the possibility of a meta-stable cis configuration at $\theta \simeq 40°$. It thus appears that the addition reaction of Al to acetylene is symmetry restricted to yield only the cis form, and a barrier exists to prevent the conversion to the more stable trans isomer. The barrier need not be much higher than kT of the colliding atom/molecular beams since the conversion would be a unimolecular process at extremely low pressure ($\leq 10^{-5}$ torr), and the adduct remains at ambient temperature for only $\sim 10^{-5}$ s. Most interestingly, the EHT calculation (Figure 13) also showed that the cis-to-trans conversion should lead to a decrease of ~20 G in the isotropic Al coupling constant as observed experimentally.

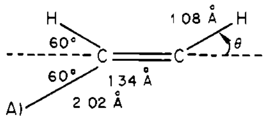

Acknowledgment. The author wishes to express his sincere appreciation to D. McLeod, Jr. (Union Carbide Corporation, Tarrytown, NY), for his assistance in obtaining many of the experimental results presented in this paper.

Registry No. Al, 7429-90-5; C_2H_4, 74-85-1; C_2D_4, 683-73-8; C_2H_2, 74-86-2; C_2D_2, 1070-74-2.

Deuterium Nuclear Quadrupole Resonance Spectra of Nonlinear Hydrogen Bonds

Theodore L. Brown,* Leslie G. Butler, David Y. Curtin,* Yukio Hiyama, Iain C. Paul,* and Roxy B. Wilson

Contribution from the School of Chemical Sciences and Materials Research Laboratory, University of Illinois, Urbana, Illinois 61801. Received July 6, 1981

Abstract: The ^2H NQR spectra of several compounds having nonlinear hydrogen bonds (O–H···O angle of less than 150°) have been obtained at 77 K by a field-cycling double-resonance method: 1,3-diphenyl-1,3-propanedione, salicylamide, 1,4-dihydroxyanthraquinone, tropolone, salicyclic acid, 2-nitrophenol, 1-hydroxy-9-fluorenone, 3-hydroxy-2-naphthoic acid, and 1-hydroxy-2-naphthoic acid. The values obtained for the quadrupole coupling constants are higher than those found in a linear hydrogen bond of the same O···O distance. A single-crystal NMR study of 1,3-diphenyl-1,3-propanedione has been carried out at room temperature by a rotating-frame double-resonance experiment. The results show that the principal (z) axis of the deuterium electric field gradient tensor lies nearly along the O–H bond direction. Additional ^2H NQR spectra for several linear hydrogen-bonded systems in the crystalline benzoic acid, 4-chlorobenzoic acid, 2-bromobenzoic acid, 3-hydroxybenzoic acid, potassium acid phthalate, salicylamide, 3-hydroxy-2-naphthoic acid, and 1-hydroxy-2-naphthoic acid, have also been obtained. In addition, an X-ray structural study of 1-hydroxy-9-fluorenone has provided structural data to test for enhancement of the ^2H quadrupole coupling constant for the case of a relatively long nonlinear hydrogen bond.

Hydrogen bonding is widely recognized to be a fundamental feature of chemical and biological systems.[1-3] Numerous experimental techniques, including X-ray and neutron diffraction, infrared spectroscopy, and nuclear magnetic resonance spectroscopy, have been applied to the study of hydrogen bonding in solids. To a limited extent, deuterium nuclear quadrupole resonance (NQR) has also been employed. The results obtained thus far have demonstrated that the deuterium quadrupole constant (DQCC) is very dependent upon the hydrogen bond geometry,[4-10] and motional effects.[4,11-13] However, little work has been done on very short (O···O distance less than 2.55 Å) or highly nonlinear hydrogen bonds (O–H···O bond angle less than 150°). Neither have there been any reports of the use of nuclear quadrupole double resonance by level crossing (ADLF)[14,15] to study motional effects in the solid state.

We report the ^2H NQR data for a variety of hydrogen-bonded systems in the solid state as determined by the ADLF technique and the X-ray structure of 1-hydroxy-9-fluorenone, one of the substances studied by this method. The ^2H NQR data are interpreted in terms of the hydrogen bond geometry. In addition, we have completely determined the orientation of the electric field

---

(1) Pimentel, G. C.; McClellan, A. L. "The Hydrogen Bond"; W. H. Freeman and Co.: San Francisco, 1960.

(2) Hamilton, W. C.; Ibers, J. A. "Hydrogen Bonding in Solids"; W. A. Benjamin: New York, 1968.

(3) Schuster, P., Zündel, G., Sandorfy, C., Eds. "The Hydrogen Bond"; North-Holland Publishing Co.: Amsterdam, 1976; Vols. I, II, and III.

(4) Chiba, T. *J. Chem. Phys.* **1963**, *39*, 947.

(5) Soda, G.; Chiba, T. *J. Phys. Soc. Jpn.* **1969**, *26*, 249.

(6) Soda, G.; Chiba, T. *J. Chem. Phys.* **1969**, *50*, 439.

(7) Hunt, M. J.; Mackay, A. L. *J. Magn. Reson.* **1974**, *15*, 402.

(8) Berglund, B.; Vaughan, R. W. *J. Chem. Phys.* **1980**, *75*, 2037.

(9) Berglund, B.; Lindgren, J. *J. Mol. Stuct.* **1978**, *179*, 43.

(10) Butler, L. G.; Brown, T. L. *J. Am. Chem. Soc.* **1981**, *103*, 6541.

(11) Blinc, R., ref 3, Chapter 18.

(12) Looyestijn, W. J.; Klaassen, T. O.; Poulis, N. J. *Physica B + C (Amsterdam)* **1979**, *96B + C*, 303.

(13) Berglund, B.; Eriksson, A.; Lindgren, J.; Tegenfeldt, J. *J. Mol. Struct.* **1979**, *52*, 113.

(14) Edmonds, D. T. *Phys. Rep.* **1977**, *29C*, 233.

(15) Rubenacker, G. V.; Brown, T. L. *Inorg. Chem.* **1980**, *19*, 392.

0002-7863/82/1504-1172$01.25/0